Title: Magnetically guided protein transduction by hybrid of nanogel chaperone with iron oxide nanoparticles

Authors: Riku Kawasaki; Yoshihiro Sasaki, Dr.; Kiyofumi Katagiri; Sada-atsu Mukai; Shinichi Sawada; Kazunari Akiyoshi

To be cited as: 10.1002/anie.201602577

Link to VoR: http://dx.doi.org/10.1002/anie.201602577

Magnetically guided protein transduction by hybrid of nanogel chaperone with iron oxide nanoparticles

Riku Kawasaki, Yoshihiro Sasaki*, Kiyofumi Katagiri, Sada-atsu Mukai, Shin-ichi Sawada and Kazunari Akiyoshi*

Abstract: Protein pharmaceuticals show great therapeutic promise, but effective intracellular delivery remains challenging. To address the need for efficient protein transduction systems, we used a magnetic nanogel chaperone (MC): a hybrid of a polysaccharide nanogel, a protein carrier with molecular chaperone-like properties, and iron oxide nanoparticles, enabling magnetically guided delivery. The MC complexed with model proteins, such as BSA and insulin, and was not cytotoxic. Cargo proteins were delivered to the target HeLa cell cytosol using a magnetic field to promote movement of the protein complex toward the cells. Delivery was confirmed by fluorescence microscopy and flow cytometry. Delivered β-galactosidase, inactive within the MC complex, became enzymatically active within cells, to convert a prodrug. Thus, cargo proteins were released from MC complexes via exchange interactions with cytosolic proteins. The MC is a promising tool for realizing the therapeutic potential of proteins.

Protein pharmaceuticals are promising for combating human diseases including cancer, metabolic disorders and autoimmune diseases.[1] More than 130 proteins or peptides have been approved for clinical use.[2] Compared with conventional small molecule drugs, protein pharmaceuticals have several advantages, derived from their specific and multiple functions and high biocompatibility.[1] Furthermore, therapy with proteins can avoid issues encountered with other types of agents, such as permanent or random genetic alterations of cells caused by nucleic acid drugs. Thus, protein pharmaceuticals, which have only temporary therapeutic effects, are often safer and more efficient alternatives than gene therapies.[1]

Despite their fascinating potential, protein pharmaceutical development remains challenging because of their physical and chemical instabilities, necessitating high doses. To date, many nanocarriers for protein pharmaceuticals have been designed and synthesized, including lipids,[3] polymers,[4] nanogels[5] and inorganic nanoparticles.[6] In addition, most protein pharmaceuticals (*e.g.*, antigens, cytokines and transcription factors) exert their functions by binding to the cell membrane surface or to extracellular targets.[1] However, recent progress in molecular biology has indicated that intracellular delivery of proteins could increase their potential uses in cancer therapy or regenerative medicine.[2] Accordingly, effective systems for delivery of proteins into the cell, that is, protein transduction systems,[17] are needed to fully realize the therapeutic potential of proteins.

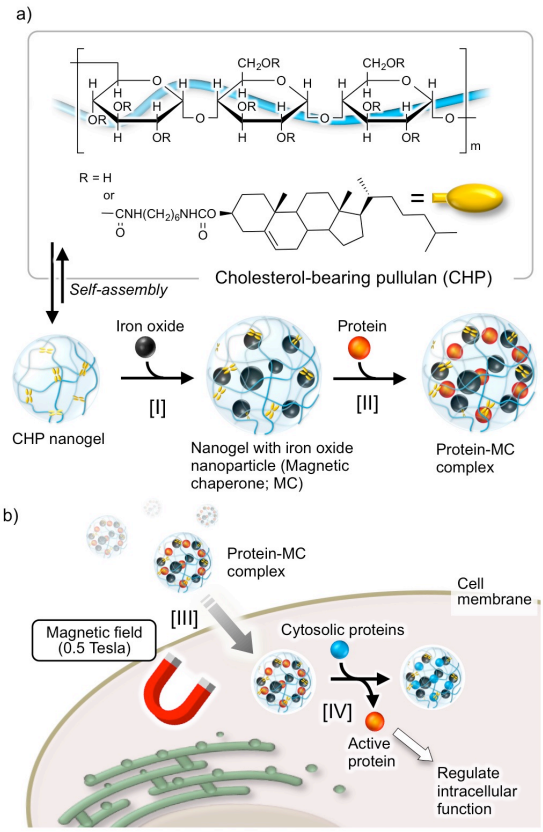

Figure 1. Design of a magnetically guided protein transduction system. a) Preparation of protein/MC complexes. [I] The MC was prepared by mixing a nanogel with hydrophobized iron oxide nanoparticles [II] Proteins were encapsulated within the polymer matrix of MC. b) Delivery of proteins by MC to the cytosol. [III] Movement of protein/MC complexes toward cells, guided by an external magnetic field. [IV] Release of proteins within the cell by exchange reactions of cargo proteins with cytosolic proteins.

Recently, many nanocarriers with magnetic properties have been developed to achieve efficient intracellular drug delivery. For instance, magnetic nanoparticles coated with lipid,[8] polymers[9] and proteins[10] were designed as magnetically guided delivery systems. In particular, transfection methods using magnetic nanoparticles, known as magnetofection,[11] have been extensively investigated and their efficiencies confirmed in various cell lines. However, few examples have been described using covalent attachment of proteins to magnetic nanoparticles in magnetically guided protein delivery systems[12] because maintaining proteins in their innate and functional form would be difficult to achieve with such approaches.[13]

[*] R. Kawasaki, Dr. Y. Sasaki, Dr. S. Mukai, Dr. S. Sawada, Prof. Dr. K. Akiyoshi
Department of Polymer Chemistry, Graduate School of Engineering, Kyoto University Katsura, Nishikyo-ku, Kyoto (Japan)
E-mail: akiyoshi@bio.polym.kyoto-u.ac.jp
Dr. K. Katagiri
Graduate School of Engineering, Hiroshima University 1-4-1 Kagamiyama, Higashi-Hiroshima (Japan)
Dr. S. Mukai, Dr. S. Sawada, Prof. Dr. K. Akiyoshi
JST-ERATO, Akiyoshi Bio-nanotransporter Project, Kyoto University Katsura, Nishikyo-ku, Kyoto (Japan).

Supporting information for this article is available via a link at the end of the document.

To address these issues in protein transduction, two approaches were employed here. One was to develop techniques to handle proteins, inspired by molecular chaperones. The chaperone-like function is defined as one that traps proteins without causing their aggregation and releases them in native form. This is an important concept for the formulation of a protein pharmaceutical. The other approach employed here was efficient intracellular delivery using an external magnetic field, which is generally harmless to both recipient cells and cargo proteins. The basic idea for magnetically guided protein transduction is shown in Figure 1. Specifically, magnetically guided nanocarriers were designed and synthesized by hybridizing an amphiphilic polysaccharide nanogel with magnetic nanoparticles. The hybrid (magnetic nanogel chaperone, MC) was anticipated to have both the function of a nanogel as a protein nanocarrier and magnetic properties.

We have developed physically crosslinked nanogels as protein nanocarriers.[14] For example, hydrophobic polysaccharides, such as cholesterol-bearing pullulan, form self-assembled nanogels in water via physical crosslinking by hydrophobic cholesterol groups.[15] One of the most attractive characteristics of the nanogels is their molecular chaperone-like function, enabling capture of proteins within their polymer matrix via hydrophobic interactions. In addition, the dynamic properties of self-assembled nanogels enable release of the proteins from the nanogel via exchange reactions with other proteins in the bulk phase.[14a] The “catch and release” chaperone function allowed nanogels to act as protein nanocarriers in the development of a cancer vaccine (in Phase 1 and 2 clinical trials), a nasal vaccine,[16] and delivery systems for cytokines such as interleukin-1[17] and bone morphogenetic protein.[18] We previously reported facile preparation of hybrids of nanogels and iron oxide nanoparticles with excellent theranostic properties including T_2 relaxivity, for use as a magnetic resonance imaging (MRI) contrast agent, and a heat generator, for magnetic hyperthermia.[19] These preliminary results encouraged us to develop a nanocarrier to deliver protein pharmaceuticals into cells using an external magnetic field, which can induce movement of the nanocarrier toward targeted cells to deliver the cargo proteins within.

Preparation and detailed characterization of the hybrid were reported elsewhere.[18] Briefly, the hybrid was prepared by mixing an aqueous nanogel suspension formed with cholesterol-bearing pullulan (CHP) (100 μg mL^{-1}) and an aliquot of hydrophobized iron oxide nanoparticles suspended in tetrahydrofuran[19] (The hydrodynamic diameter of the magnetic nanoparticles was 12 nm and their polydispersity index was 0.012).

At first, to examine the appropriateness of the MC as an intracellular delivery carrier, viability of HeLa cells in the presence of the MC was evaluated using a modified MTT assay. Figure 2a shows the viability of cells treated with a pure CHP nanogel (100 μg mL^{-1}) or a CHP nanogel (100 μg mL^{-1}) mixed with 1, 10 or 100 μg mL^{-1} iron oxide nanoparticles (MC1, 10, and 100, respectively, Figure S1, and Table S1). No apparent cytotoxicity was observed even at the highest concentration of iron oxide nanoparticles after irradiation of magnetic field for 24 h. This suggests that the MC could be used as non-toxic nanocarrier, even under magnetic field irradiation.

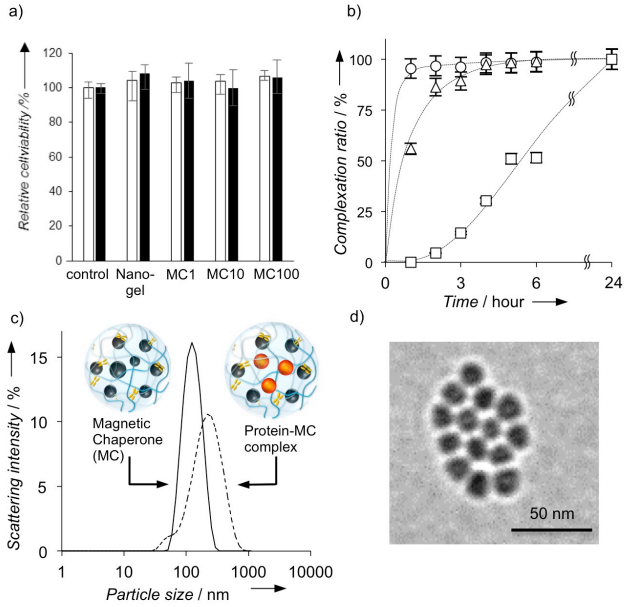

Figure 2. Characterization of MC and its interactions with proteins. a) Cytotoxicity of MC in the absence (white) or presence (black) of a magnetic field. HeLa cells were treated with CHP nanogel or MC. The concentration of CHP nanogel was fixed at 100 μg mL^{-1}. Three independent experiments were performed in triplicate. b) Complexation between MC (100 μg mL^{-1}), open circle; MC1, open triangle; MC10, open square; MC100) and Alexa488-labeled BSA (17 μg mL^{-1}), which were estimated by fluorescence spectroscopy after magnetic separation. Three independent experiments were performed in triplicate c) Size distribution of MC1 and MC1/BSA complexes. MC was dispersed in PBS (25 °C, pH 7.4). d) Transmission electron microscopic images of MC1/BSA complex (MC1, 100 μg mL^{-1}; BSA: 17 μg mL^{-1}) in PBS, scale bar indicates 50 nm.

Protein complexation with the MC was evaluated using fluorescently labeled bovine serum albumin (BSA, 68 kDa) as a model protein. BSA (17 μg mL^{-1}) was incubated with MC (100 μg mL^{-1}) for 24 h. Proteins incorporated with the MC were separated from free proteins in a magnetic field and the fluorescence intensity of the supernatant was measured to quantify the complexation ratio (%), expressed as the amount of incorporated protein relative to the total protein (Figure 2b). When BSA was mixed with MC1, all protein was incorporated into the nanogel within 3 h. In addition, the complexation rates depended on the ratio of nanogel to iron oxide nanoparticles, indicating that the protein binding capacity of the MC can be tuned by changing the incorporated concentration of iron oxide nanoparticles.

Dynamic light scattering analysis showed that the size of the MC1 increased from 100 to 180 nm after complexation with BSA (Figure 2c). However, the zeta-potential did not significantly change (from −1.0 to −0.4 mV), although MC

interacted with anionic BSA under the pH conditions applied. These results indicate that BSA was encapsulated within the nanogel, shielding its anionic charge. Figure 2d shows representative morphological images of a MC/BSA complex observed by transmission electron microscopy, indicating that MCs maintained their spherical morphology after complexation with proteins.[17]

Performance of MC as a magnetically guided intracellular protein nanocarrier was investigated by confocal laser scanning microscopy (CLSM). HeLa cells were exposed to a MC/BSA complex (100 μg mL^{-1}; BSA: 17 μg mL^{-1}) for 24 h and magnetic fields (c.a. 0.5 T) were applied towards the cells from the bottom of the culture dish. The subcellular distributions of delivered carriers and fluorescence-labeled cargo proteins were observed by CLSM. Fluorescence from MC (red) and BSA (green) were detected in the cytosol when magnetically induced protein delivery was performed with MC1 (Figure 3a and S2c). In contrast, fluorescence was not detected in cells incubated with conventional nanogels, or with MC1 in the absence of a magnetic field (Figure S1). Flow cytometry also showed that proteins were effectively delivered by MC under a magnetic field (Figure 3b).

The intracellular uptake efficiency of MC under the influence of a magnetic field depended on the strength and direction of the magnetic field toward the cells (Figure S3). The magnetically induced protein delivery systems with MC yielded, on average, a 100-fold enhancement of MC and BSA uptake compared with the same carrier in the absence of a magnetic field. The fluorescence from MC1 and cargo proteins dispersed separately in the cytosol after 24 h. In addition, the cellular uptake was not inhibited by incubation at 4 °C (Figure S4), suggesting that MCs were taken up by following two energy-independent pathways. One is direct crossing of the plasma membrane by spearing the lipid bilayer and the other is endocytosis-like uptake resulting from magnetic energy. To further examine the release of proteins from MCs, the co-localization of MC and BSA was estimated. As expected, the co-localization ratio was decreased from 80% at 4 h to 30% at 24 h. These results indicate that the proteins were released from MC within cells after 24 h, because of an exchange reaction between cargo and cytosolic proteins.

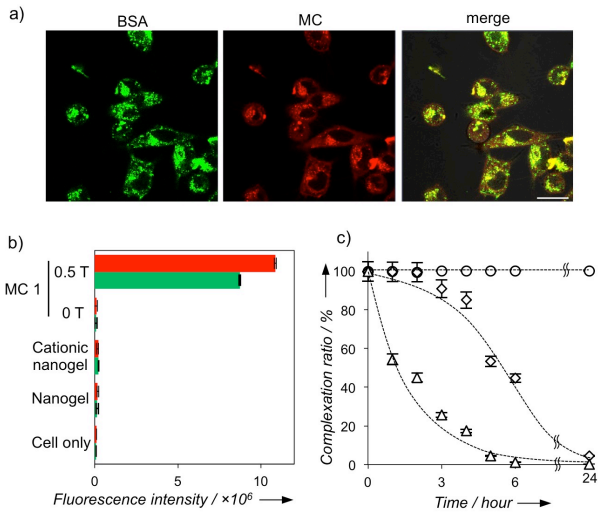

Figure 3. Cell uptake of MC/Alexa488-BSA complexes under irradiation in a magnetic field. a) Confocal laser scanning microscopic images of HeLa cells after incubation for 24 h with a complex of rhodamine B-labeled MC1 with Alexa488-labeled BSA under a magnetic field (MC1, 100 μg mL^{-1}; BSA, 17 μg mL^{-1}). The scale bar indicates 20 μm. b) Mean fluorescence of rhodamine B-labeled MC1 (red) or Alexa488-labeled BSA (green) accumulated in HeLa cells, as determined by flow cytometry after 24 h incubation with nanogel/BSA complexes, or MC1/BSA complexes. c) Protein release in FBS, mimicking the intracellular environment. After complexation with BSA, PBS (○) or FBS (10%◇, 20%△) were added to the complex and labeled protein release was determined by fluorescence spectroscopy after magnetic separation. Three independent experiments were performed in triplicate.

To demonstrate protein release from MC, MC/BSA complex (MC1, 100 μg mL^{-1}; BSA, 17 μg mL^{-1}) was co-incubated with highly concentrated serum proteins. Release of incorporated proteins was quantified after magnetic separation of complexed protein to free protein. As shown in Figure 3c, BSA was not released from MC in PBS, whereas BSA was gradually released from MC in the presence of concentrated serum proteins in fetal bovine serum (FBS). The protein release efficiency was accelerated by increasing the concentration of serum proteins with FBS (10% FBS to 20% FBS). The serum proteins were detected in MC after mixing with FBS and incubation for 24 h by polyacrylamide gel electrophoresis (SDS-PAGE, Figure S5). These results indicate that the cargo proteins were replaced with serum proteins via an exchange reaction. Generally, the cytosol is filled with highly concentrated proteins. Accordingly, MC released cargo proteins within the cytosol through a protein exchange reaction. Similar protein release was observed with insulin as a lower molecular weight model protein (Figure S6).

The function of proteins delivered by MC to the cytosol was investigated with a hydrolytic enzyme, β-galactosidase (β-gal). When a solution of β-gal (0.42 μg mL^{-1}) and MC (100 μg mL^{-1}) was incubated for 24 h, 52% of β-gal was complexed with MC. The MC/β-gal complex was then separated from free β-gal and its enzymatic activity evaluated by monitoring the hydrolysis of the galactosyl moiety of non-fluorescent Tokyo-green β-gal (10 nM) to fluorescent Tokyo-green. As shown in Figure 4a, β-gal was inactivated by complexation with MC. After addition of FBS to the complex, however, β-gal recovered its enzymatic activity, probably because of its release and refolding via protein exchange reactions with serum proteins in FBS. These results showed that MC acted as an artificial molecular chaperone, enabling it to catch and release cargo proteins via exchange reactions with cytosolic proteins.

Protein transduction efficiencies were directly evaluated by monitoring enzymatic activity of MC-delivered β-gal within Hela cells. The complex of β-gal with MC was incubated with Hela cells for 24 h under a magnetic field

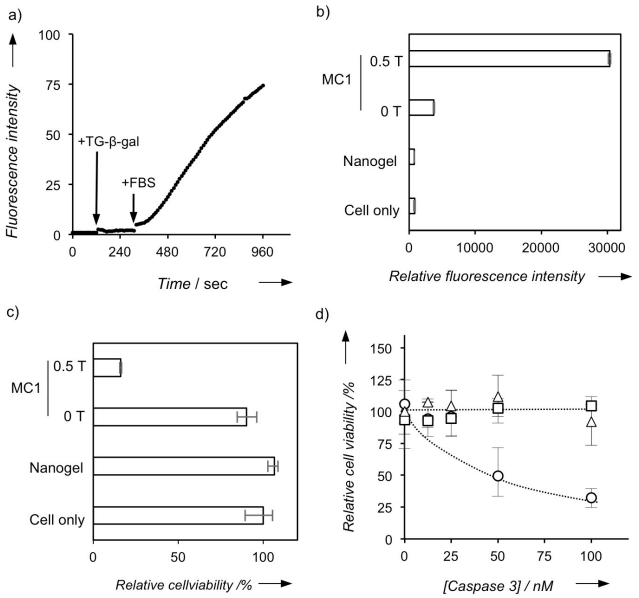

Figure 4. Chaperone like activity of MC via protein exchange reactions and protein transduction using MC. a) Recovery of enzymatic activity of β-gal after its release from MC. MC/β-gal complex was mixed with Tokyo green β-gal (10 nM) and 20% FBS. Each reagent was added at 60 or 300 sec. b) Protein transduction efficiencies, determined by measuring fluorescence intensity of Tokyo green β-gal. HeLa cells were incubated with nanogel/β-gal complex, MC1/β-gal complex, or MC1/β-gal complex under magnetic field. The concentration of β-gal was fixed at 0.42 μg mL^{-1}. Tokyo green β-gal (10 μM) was added after 24 h incubation. c) Activation of the anticancer prodrug 5-FUR-β-gal by MC/β-gal complexes, as determined by HeLa cell viability. Relative cell viabilities were determined after treatment 24 h with nanogel/β-gal complexes, MC1/β-gal complexes in the presence of magnetic field or absence of an external magnetic field. Three independent experiments performed in triplicate. The concentration of nanogel and β-gal were fixed at 10 μg mL^{-1} and 0.42 μg mL^{-1}, respectively. The standard deviations of three independent measurements are shown. Three independent experiments performed in duplicate. d) Delivery of caspase 3 into CT26 cells. CT26 (murine colon cancer cells) were treated with free caspase 3 (open square), MC/caspase 3 without irradiation of magnetic field (open triangle), and with irradiation of magnetic field (open circle). After 24 h, cell viabilities were evaluated by WST-8 assay. The concentration of MC was fixed at 100 μg mL^{-1}. Three independent experiments performed in triplicate

and then CLSM observation was carried out. No fluorescence was detected in the case of free β-gal, the nanogel/β-gal complex, and the MC/β-gal complex without a magnetic field (Figure S7). However, when β-gal was delivered within HeLa cells using MC under a magnetic field, the fluorescence from Tokyo green, which was generated by the hydrolysis of Tokyo-green β-gal, was clearly observed throughout the cytosol (Figure S7d or f). In contrast, lower fluorescence emission from Tokyo green was observed when β-gal was delivered from a cationic nanogel as a positive control.

The enzymatic activity was also quantified by flow cytometry. Fluorescence intensity from cells treated with a MC1/β-gal complex under a magnetic field was 100 times higher than without a magnetic field (Figure 4b). The enzymatic activity within cells gradually decreased, over 72 h, to 8.5% (Figure S8). The disappearance of protein activity within cells is advantageous for protein therapies that require temporal pharmaceutical effects.

A prodrug assay was conducted using β-gal conjugated with cytotoxic 5-fluorouridine (5-fluorouridine-5′-*O*-β-galactopyranoside, 5-FUR-β-gal) as a model prodrug substrate. When the galactosyl moiety of 5-FUR-β-gal was hydrolyzed by β-gal, the product 5-FUR showed dose-dependent cytotoxicity, whereas 5-FUR-β-gal was not cytotoxic (Figure S9). After magnetically guided protein transduction using MC, an apparent cytotoxicity from 5-FUR for Hela cells was observed (Figure 4c). Thus, the delivered β-gal showed enzymatic activity within cells to convert non-cytotoxic 5-FUR-β-gal into cytotoxic 5-FUR.

Finally, the utility of MC for DDS was assessed by delivering caspase 3, which is a known cytosolic protease that participates in a signaling pathway leading to programed cellular death (apoptosis). The caspase 3 or MC/caspase 3 complex was incubated with murine colon cancer cells (CT26 cells) for 24 hr. An apparent cytotoxicity was observed only when caspase 3 was delivered by MCs under the influence of a magnetic field (Figure 4d). In addition, it was proven using flow cytometry that cell destruction was induced through an apoptosis pathway by the delivered caspase 3 (Figure S10).

In conclusion, we demonstrated a facile magnetically guided protein transduction method using polysaccharide nanogels with iron oxide nanoparticles. The chaperone-like function of nanogels and the magnetic properties of iron oxide enabled highly efficiency delivery of proteins in their active forms to target cells. Consequently, our strategy has great potential as a key technique for protein transduction. We believe that supramolecular chemistry-based approaches such as ours have unique features applicable to delivering a wide range of proteins for protein-based therapies or regenerative medicine in the near future.

Acknowledgements

This work was supported by the Exploratory Research for Advanced Technology division of the Japan Science and Technology Agency (JST-ERATO).

Keywords: drug delivery · protein transduction • physical crosslinked nanogels • organic–inorganic hybrid nanomaterials• protein based therapy

References

[1] Y. Lu, W. Sun, Z. Gu, *J. Contr. Rel.*, **2014**, *194*, 1.
[2] B. Leader, Q. J. Baca, E. Golan, *Nat. Rev. Drug Discov.,* **2008**, 7, 21.
[3] M. Wang, K. Alberti, S. Sun, C. L. Arellano, Q. Xu, *Angew. Chem. Int. Ed.*, **2014**, *53*, 2893.
[4] a) Y. Wu, D. Y. W. Ng, S. L. Kuan, T. Weil, *Biomater. Sci.*, **2015**, *3*, 214; b) A. Biswas, Y. Liu, T. Liu, G. Fan, Y. Tang, *Biomaterials,* **2012**, *33, 21*, 5459; c) M. Zhao, Y. Liu, R. S. Hsieh, N. Wang, W. Tai, K.-I. Joo, P. Wang, Z. Gu, Yi Tang, *J. Am. Chem. Soc.* **2014**, *136*, 15319.
[5] a) Y. Sasaki and K. Akiyoshi, *Chem. Rec.*, **2010**, *10*, 366; b) K. S. Soni, S. S. Desale, T. K. Bronich, *J. Contr. Rel.*, **2016**, *in press.*

[6] a) I. I. Slowing, B. G. Trewyn, and V. S.-Y. Lin, *J. Am. Chem. Soc.* **2007**, *129*, 8845.: b) X. Wu, Y. Song, J. Han, L. Yang, and S. Han, *Biomaterials science*, **2013**, *1*, 918.: c) R. Tang *et. al., ACS Nano*, **2013**, *7*, 6667.
[7] D. S. D' Astolfo, R. J. Pagliero, A. Pras, W. R. Karthaus, H. Clecers, V. Prasad, R. J. Lebbink, H. Rehmann, and N. Geijisen, *Cell*, **2015**, *161*, 674.
[8] R. D. Corato, G. Bealle, J. Kolosnjaj-Tabi, A. Espinosa, O. Clement, A. K. A. Silva, C. Menager, C. Wilhelm, *ACS Nano*, **2015**, *9, 3,* 2904.
[9] a) J. Zhang, S. Zhao, M. Zhu, Y. Zhang, Z. Liu, C. Zhang, *J. Mater. Chem. B*, **2014**, *2*, 7583; b) J. Li, Y. Hu, J. Yang, P. Wei, W. Sun, M. Shen, G. Zhang, X. Shi, *Biomaterials*, **2015**, *38*, 10.
[10] T. T.-D. Tran, T. V. Vo, P. H. L. Tran, *Chem. Engr. Res. and Des.*, **2015**, *94*, 112.
[11] J Dobson, *Gene Ther.,* **2006**, *13*, 283.
[12] a) X. Luo, S. Liu, J. Zhou and L. Zhang, *J. Mater. Chem.*, **2009**, *19*, 3538; b) Z. Wang, J. Zhang, R. Li, J. Chen, *J. Appl. Polym. Sci.*, **2014**, *10*, 40260.
[13] J. Gao, W. Zhang, P. Huang, B. Zhang, X. Zhang and B. Xu, *J. Am. Chem. Soc.* **2008**, 130, 3710.
[14] a) Y. Sasaki, K. Akiyoshi, *Curr. Pharm. Biotechnol.* **2010**, *11*, 814; b) H. Ayame, N. Morimoto, K. Akiyoshi, *Bioconj. Chem*, **2008**, *19*, 882; c) A. Shimoda, S. Sawada, K. Akiyoshi. *Macromol. Biosci*., **2011**, *117*, 882.
[15] K. Akiyoshi, S. Deguchi, N. Moriguchi, S. Yamaguchi, J. Sunamoto, *Macromolecules*, **1993**, *26*, 3062.
[16] T. Nochi, *et al. Nat. Mater.*, **2010**, *9*, 572.
[17] a) T. Shimizu, T. Kishida, U. Hasegawa, Y. Ueda, J. Imanishi, H. Yamagishi, K. Akiyoshi, E. Otsuji, O. Mazda, *Biochem. Biophys. Res. Commun.*, **2008**, *367*, 330; b) U. Hasegawa, S. Sawada, T. Kishida, E. Otsuji, O. Mazuda, K. Akiyoshi, *J. Contr. Rel.*, **2009**, *140*, 312.
[18] M. Fujioka-Kobayashi, M. S. Ota, A. Shimoda, K. Nakahama, K. Akiyoshi, Y. Miyamoto, S. Iseki, *Biomaterials*, **2012**, *33*, 7613.
[19] K. Katagiri, K. Ohta, K. Sako, K. Inumaru, K. Hayashi, Y. Sasaki, K. Akiyoshi, *ChemPlusChem*, **2014**, *79*, *11*, 1631.

Entry for the Table of Contents

COMMUNICATION

Magnetic chaperone protein transduction: Facile protein transduction was achieved using a hybrid of polysaccharide nanogels with iron oxide nanoparticles. The chaperone-like functions of the nanogel and magnetic properties of the iron oxide nanoparticles enabled delivery of functional proteins, while maintaining their innate activities, into target cells.

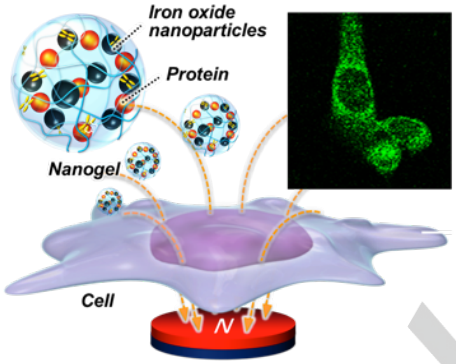

Riku Kawasaki, Yoshihiro Sasaki, Kiyofumi Katagiri, Sada-atsu Mukai, Shin-ichi Sawada, and Kazunari Akiyoshi**

Page No. – Page No.

Magnetically guided protein transduction by a hybrid of a nanogel chaperone with iron oxide nanoparticles

Angewandte Chemie
Eine Zeitschrift der Gesellschaft Deutscher Chemiker

Supporting Information

Magnetically guided protein transduction by hybrid of nanogel chaperone with iron oxide nanoparticles

Riku. Kawasaki[a,c], Yoshihiro. Sasaki[a], Kiyofumi. Katagiri[b], Sada-atsu. Mukai[a,c], Shin-ichi. Sawada[a,c] and Kazunari. Akiyoshi[a,c]

1. Materials and methods

Materials. Cholesterol-bearing pullulan (CHP), in which the pullulan (*M*w, 1.0×10^5 g mol^{-1}) was substituted with 1.3 cholesteryl ester groups per 100 glucose units, was a gift from Nippon Oil and Fat Corporation (Tokyo, Japan). Alexa fluor 488-labeled bovine serum albumin (Alexa488-BSA, 68 kDa), Fluorescein isothiocyanate-labeled insulin (FITC-insulin, 28 kDa) and β-galactosidase from *Escherichia coli.* (β-gal, 168 kDa) were from Sigma-Aldrich (St. Louis, MO, USA). TokyoGreen-β-Gal, 5-fluorouridine (5-FUR), and 5-fluorouridine-5′-*O*-β-D-galactopyranoside (5-FUR-β-gal) were from Sekisui Medical (Tokyo, Japan), TCI (Tokyo, Japan) and Funakoshi (Tokyo, Japan), respectively. A Cell-Counting Kit-8 (CCK-8) was obtained from Dojindo Laboratories (Kumamoto, Japan).

Synthesis of rhodamine B-labeled CHP. Rhodamine B-labeled CHP (degree of substitution of the rhodamine B moiety per 100 glucose units of 0.2) was synthesized as previously described [1]. Briefly, CHP was vacuum-dried at 70 °C for 3 d. CHP, di-*n*-butytin dilaurate (DBTDL; Sigma Aldrich) and rhodamine B isothiocyanate (RITC; Sigma Aldrich) were dissolved in anhydrous dimethyl sulfoxide (DMSO). The concentrations of CHP, DBTDL, and RITC were 10 mg mL^{-1}, 20 and 2.0 mM, respectively. The resulting solution was precipitated twice into a mixture of diethyl ether and ethanol (8:2, v/v). The isolated solid material was vacuum-dried at room temperature overnight and suspended in DMSO (CHP concentration, 10 mg mL^{-1}). The suspension was dialyzed against DMSO and water. The degree of substitution of the rhodamine B to the glucose units of the pullulan was estimated using UV-vis spectroscopy (JASCO, Tokyo, Japan) at 558 nm.

Preparation of nanogel with iron oxide nanoparticles (MC). MC was prepared as previously described [2]. Briefly, CHP was suspended in Milli-Q water, and stirred overnight at room temperature. The solution was sonicated using a probe-type sonicator (Sonifier 250, Branson, Danbury, USA) at 40 W for 15 min with cooling on ice. The solution was filtered through 0.22 μm polyvinylidene difluoride filters (Millex-HV, Millipore, Bedford, MA, USA). Oleic acid coated Fe_3O_4 nanoparticles were synthesized via a conventional hydrothermal process and were purified by removing byproducts in *n*-hexane, with centrifugation. The Fe_3O_4 nanoparticles were then re-dispersed in THF (0.2, 2.0, 20 mg mL^{-1}). MC was obtained by injecting the THF suspension of the oleic acid-coated Fe_3O_4 nanoparticles into a CHP nanogel aqueous suspension with vortex mixing. The solution was lyophilized to remove THF and re-dispersed in PBS.

Basic characterization of MCs. The number of iron oxide nanoparticles incorporated into a nanogel was quantified by counting the number of iron oxide nanoparticles obtained in TEM images of MC 1, 10 or 100, respectively. (N=50)

Cytotoxicity of MC. HeLa cells were seeded on a 96-well plate (BD Falcon, New Jersey, USA) at a density of 5.0×10^3 cells/well and cultured overnight. After medium was exchanged with fresh Dulbecco's modified Eagle's medium (DMEM), the MC suspension was added to each well. After incubation for 24 h, a Cell Counting Kit-8 reagent (10 μL) was added to each well and plates were further incubated for 2 h. Absorbance at 450 nm was measured with a plate reader. Cell viability was calculated relative to that for untreated cells. This assay employed a modified MTT dye reduction assay using WST-8 (2-(2-methoxy-4-nitrophenyl)-3-(4-nitrophenyl)-5-(2,4-disulfophenyl)-2H-tetrazolium, monosodium salt) (Cell Counting Kit-8, Dojindo Laboratories), according to the manufacturer's instructions.

Complexation of proteins with MC. Protein complexation was confirmed after magnetic separation of the complex from free protein. MC and proteins (FITC-insulin, Alexa488-BSA, or β-galactosidase) were mixed and incubated for 24 h at 40 °C. The concentrations of MC, FITC-insulin, Alexa488-BSA and β-galactosidase were 100, 14, 17 and 0.42 μg mL^{-1}, respectively. At each timepoint, proteins

incorporated into MC were magnetically separated from free proteins, and the complexation ratio was determined according to the following equation:

$$Complexation\ ratio\ (\%) = (1 - f/f_0) \times 100$$

where f and f_0 are the fluorescence intensity from released proteins and whole proteins, respectively. This was assessed by measuring either fluorescence intensity in a fluorescence spectrometer (FP-6500, JASCO, Japan, Tokyo) or absorbance at 280 nm in a UV-vis spectrophotometer.

Characterization of MC/protein complexes. Dynamic light scattering and zeta-potential measurements were performed with a Zetasizer Nano instrument (Malvern Instruments, Worcestershire, U.K.) operating at a wavelength of 632.8 nm and a 173° detection angle. The hydrodynamic diameter of the MC or MC/protein complex (CHP concentration: 100 μg mL^{-1}) was determined with a Laplace inversion program. The zeta-potential measurements were performed using a capillary zeta-potential cell. The morphology of the MC/protein complex was evaluated by transmission electron microscopy (TEM) (HT-7700, Hitachi, Tokyo, Japan). TEM was performed at an acceleration voltage of 100 kV and a beam current of 20 μA. The specimens were prepared by dropping 10 μL of a MC/protein complex suspension on a grid.

Cellular uptake of proteins. HeLa cells were seeded on a 12 mm glass-bottomed dish (Iwaki, Osaka, Japan), at a density of 1.0×10^5 cells per dish, and incubated overnight. After the medium was exchanged with fresh DMEM, MC/protein complex was added to each dish. The final concentrations of MC, insulin and BSA were 100, 14 and 17 μg mL^{-1}, respectively. Next, a cylindrical NdFeB magnet (dimensions: diameter = 12 mm, height = 10 mm: field strength, 0.5 T) was placed under the glass-bottomed dish for 24 h. Cells were then washed three times with PBS, medium exchanged for fresh reduced serum medium (opti-MEM) and cells were observed by confocal laser scanning microscopy (CLSM; LSM510META, Carl Zeiss, Oberkochen, Germany). CLSM observations were performed with excitation by an argon laser (488 nm for Alexa488) or He-Ne laser (543 nm for rhodamine B). Emitted fluorescence was detected through a 503–530 nm band pass filter and a 543-nm-long pass filter. The magnetic field was applied to cells and MCs in a glass-bottomed dish or a 12-well plate using a Nd-B-Fe magnet, as shown in Figure S3c. To obtain a uniform magnetic environment for each cell, a sufficiently large magnet (length, 100 mm; width, 100 mm; height, 10 mm) was used to fully cover the glass-bottomed dish or 12-well plate.

Flow cytometry. HeLa cells were seeded on a 12-well plate at a density of 1.0×10^5 cells per well and incubated overnight. After the medium was exchanged for fresh DMEM, MC/protein suspension was added to each well. The final concentrations of MC, insulin, and BSA were 10, 1.4 and 1.7 μg mL^{-1}, respectively. Next, a cylindrical NdFeB magnet (dimensions: diameter = 12 mm, height = 10 mm: field strength, 0.5 T) was placed under the glass bottom dish for 24 h. Cells were then washed three times with PBS, trypsinized and suspended in staining buffer (BD PharMingen, New Jersey, USA). Flow cytometry was performed with a Cytomix FC500 (Beckman Coulter, California, USA) with a 488 nm He-Ne laser. Signals from the FL1 band pass emission were used for FITC or Alexa488.

Protein release from MC in the presence of FBS. MC/protein complex (MC, 100 μg mL^{-1}; insulin, 1.4 μg mL^{-1}; BSA, 1.7 μg mL^{-1}) was incubated with serum proteins (PBS, 10% FBS, or 20% FBS in PBS) for 24 h. At each timepoint, MC/protein complex was separated from released proteins under a magnetic field (0.5 T) and the complexation ratio (%), as a relative amount of released protein to total protein, was calculated by measuring the fluorescence intensity of FITC or Alexa488 in the released protein fraction. In addition, encapsulation of serum proteins contained in FBS was confirmed by polyacrylamide gel electrophoresis. The gel was stained by Coomassie brilliant blue (CBB) and detected by an LAS luminescence imaging system (LAS 4000 mini, Fujifilm, Tokyo, Japan).

Enzymatic activity of β-galactosidase. The enzymatic activity of β-galactosidase was evaluated using Tokyo-green β-gal as a substrate. Non-fluorescent Tokyo-green β-gal is converted to fluorescent Tokyo-green by a hydrolytic reaction catalyzed by β-galactosidase. The fluorescence of Tokyo-green was measured in a fluorescence spectrometer (excitation at 490 nm, emission at 510 nm). The MC/β-galactosidase complex (MC, 100 μg mL^{-1}; β-galactosidase, 0.42 μg mL^{-1}) was maintained at 37 °C and its incorporated β-galactosidase was separated from free β-galactosidase under a magnetic field. Tokyo-green β-gal (10 nM) was added to the separated complex at 1 min. After 5 min incubation, serum proteins (20% FBS) were added to the solution. The enzymatic activity of β-galactosidase was estimated from the slope of the Tokyo-green signal intensity change within 15 min. The relative enzymatic activity of β-galactosidase was calculated by comparing values to the enzymatic activity of free β-galactosidase (0.42 μg mL^{-1}).

Intracellular delivery of β-galactosidase. HeLa cells were seeded on a multi-well plate at a density of 1.0×10^5 cells/well and incubated overnight. After the culture medium was removed and exchanged for fresh DMEM, the MC/β-galactosidase complex (MC, 10 μg mL^{-1}; β-galactosidase, 0.042 μg mL^{-1}) was added to each well with or without applying a magnetic field. After incubation for 24 h, cells were washed three times with PBS and Tokyo green-β-gal solution (10 μM) was added to the treated cells. After an additional 3 h, cells were washed three times with PBS, their medium was exchanged for fresh opti-MEM, and they were observed by CLSM. For flow cytometry, cells were trypsinized after Tokyo-green β-gal treatment and re-suspended in staining buffer. Flow cytometry was performed with a Cytomix FC500 (Beckman Coulter) with a 488 nm He-Ne laser. The signals from the FL1 band pass emission were used for Tokyo-green.

Prodrug assay with 5-fluorouridine-5′-*O*-β-galactopyranoside. HeLa cells were seeded on a 96-well plate (BD Falcon) at a density of 5.0×10^3 cells/well and incubated overnight. After the medium was exchanged for fresh DMEM, MC/β-galactosidase complex (MC, 10 μg mL^{-1}; β-galactosidase, 0.047 μg mL^{-1}) was added to each well with or without applying a magnetic field. After incubation for 24 h, cells were washed three times with PBS and 5-FUR-β-gal (100 μM) was applied to each well. After further incubation for 24 h, a Cell Counting Kit-8 reagent (10 μL) was added to each well and plates were incubated for 2 h. The absorbance at 450 nm was then measured with a plate reader. The cell viability was calculated relative to that of untreated cells.

Delivery of caspase 3. CT26; murine colon cancer cells were seeded on a 96-well plate at a density of 5.0×10^3 cells/well. After overnight incubation, the cell culture medium was replaced and MC/caspase 3 complex was added to the cells at various concentrations of caspase 3 with or without a magnetic field. The concentration of MC was fixed at 100 μg mL^{-1}. After 24 h incubation, cell viability was quantified with a Cell Counting Kit-8 by measuring absorbance at 450 nm using a microplate reader.

Apoptosis detection assay. CT26; murine colon cancer cells were seeded on a 96-well plate at a density of 5.0×10^3 cells/well. After overnight incubation, the cell culture medium was replaced and a MC/caspase 3 complex was added to the cells at various concentrations of caspase 3 with or without a magnetic field. The concentration of MC was fixed at 100 μg mL^{-1}. After 24 h of incubation, cells were trypsinized and re-suspended in a working mixture containing Ca^{2+} ions. After FITC-labeled annexin-V and propidium iodide (PI) were added to the suspension, the cells were analyzed using flow cytometry by detecting fluorescence from FITC or PI.

2. Basic characterization of MCs

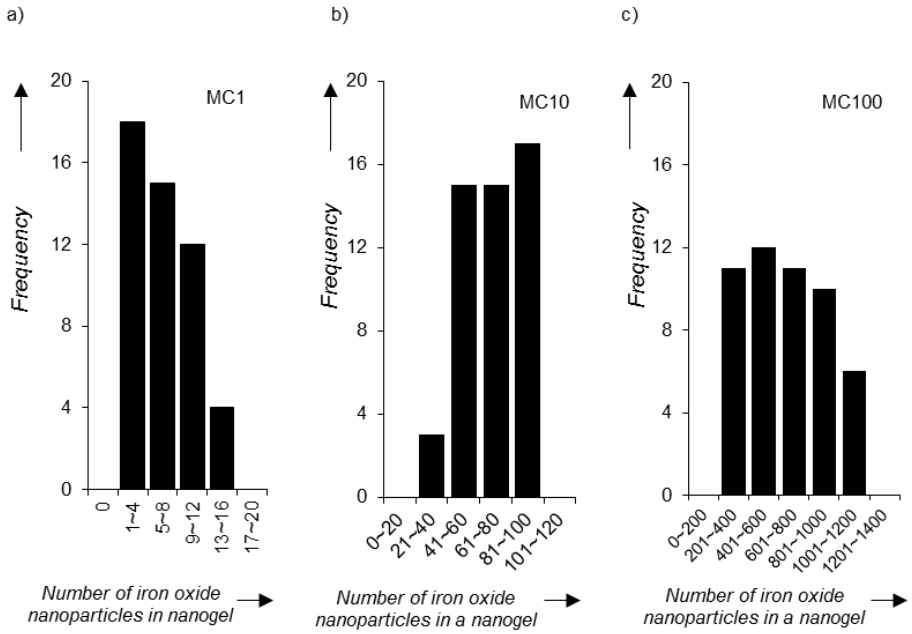

Figure S1. Histogram of the number of iron oxide nanoparticles in a nanogel (a) MC1, (b) MC10, and (c) MC100. These histograms were obtained by counting the number of iron oxide nanoparticles from TEM images of MCs. Fifty individual MCs were counted.

Table S1. The average number of iron oxide nanoparticles in a nanogel with standard deviations.

	MC 1	MC 10	MC 100
Number of iron oxide nanoparticles in a nanogel	6 ± 3.6	70 ± 22	690 ± 320

3. Size and Zeta-potential of MC and MC/protein complexes

Table S2. Hydrodynamic diameters and ζ-potentials of MC and MC/protein complexes in PBS. The particle size of MC and MC encapsulating proteins were determined by dynamic light scattering in PBS. The zeta-potentials were determined using capillary cells. PDI is the polydispersity index. The results are summarized as the mean ± standard deviation.

Sample	R_H (nm)	PDI	ζ-potential (mV)
MC1	110 ± 0	0.10 ± 0.01	−1.0 ± 0.6
MC1/insulin complex	160 ± 13	0.26 ± 0.01	0.7 ± 1.8
MC1/BSA complex	180 ± 10	0.25 ± 0.02	−0.5 ± 0.4
MC1/β-galactosidase complex	180 ± 20	0.25 ± 0.00	−0.3 ± 1.3
MC10	140 ± 20	0.06 ± 0.02	−0.0 ± 0.0
MC10/insulin complex	170 ± 20	0.24 ± 0.01	1.3 ± 0.3
MC10/BSA complex	160 ± 10	0.24 ± 0.01	−0.6 ± 1.0
MC10/β-galactosidase complex	190 ± 20	0.25 ± 0.01	0.9 ± 1.3
MC100	180 ± 0	0.04 ± 0.01	−0.5 ± 1.4
MC100/insulin complex	180 ± 10	0.25 ± 0.01	0.0 ± 0.1
MC100/BSA complex	170 ± 20	0.23 ± 0.01	−1.3 ± 0.5
MC100/β-galactosidase complex	180 ± 10	0.24 ± 0.01	−0.4 ± 2.2

4. Subcellular distribution of delivered carriers and proteins

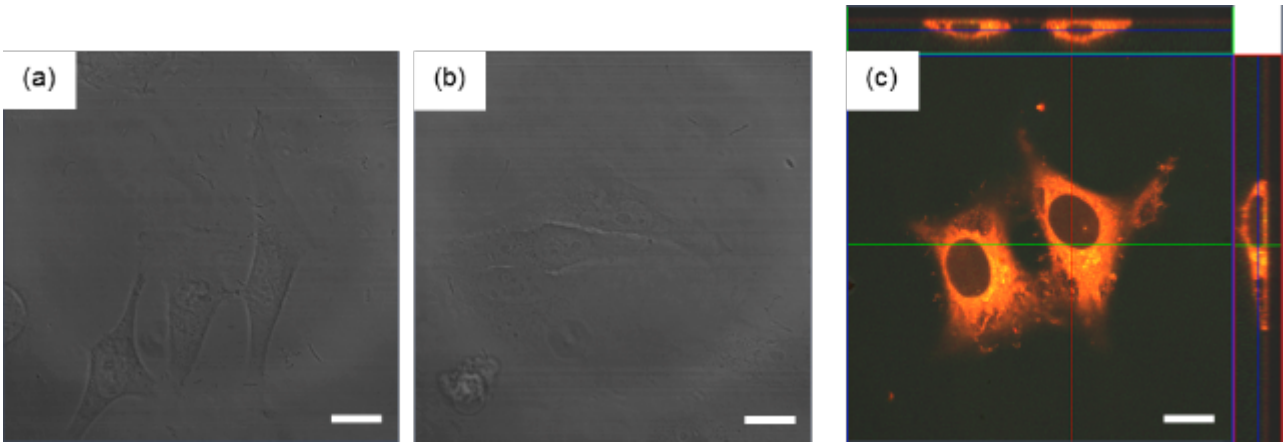

Figure S2. Interactions between nanogel/Alexa488-labeled BSA complexes and Hela cells (a) or MC1/Alexa488-labeled BSA complexes without a magnetic field (b) or MC1/Alexa488-labeled BSA complexes with a magnetic field (c). The concentrations of nanogel and BSA were 100 and 17 μg mL^{-1}, respectively. The scale bar indicates 20 μm.

5. Magnetic field dependency of magnetically guided delivery using MCs

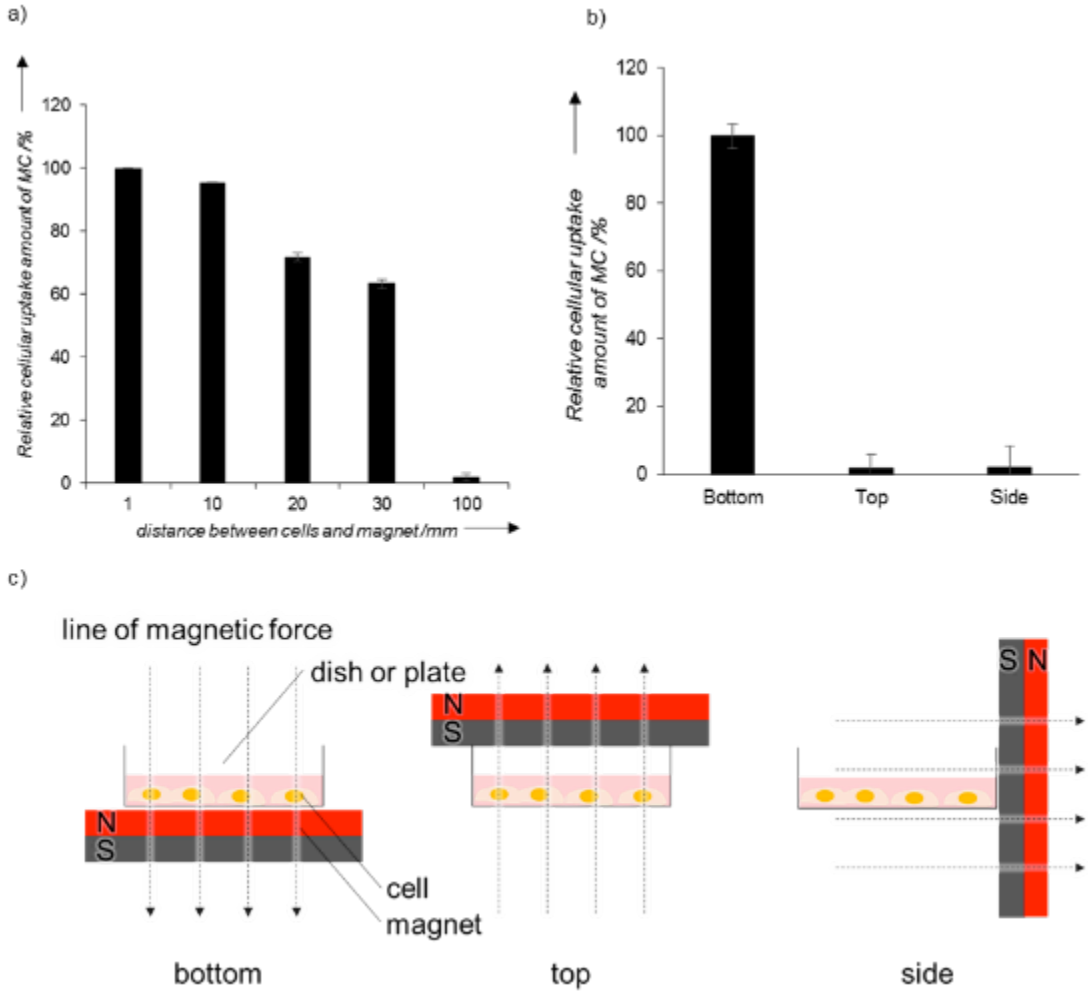

Figure S3. (a) Dependence of intracellular delivery efficiency on magnetic field intensities of MC/protein complex toward HeLa cells. Hela cells were seeded on 12-well plates (1.0×10^5 cells/well), and MC was added to cells (100 μg mL^{-1}) under the influence of various strengths of magnetic field. To produce various magnetic field strengths toward cells, the distance between cells and the magnet were varied between 1 and 100 mm. Intracellular uptake was then quantified by flow cytometry. (b) Intracellular uptake efficiencies were compared by applying magnetic fields in different orientations. The magnet was placed on the top, side or bottom of the dish. HeLa cells were seeded on 12-well plates (1.0×10^5 cells/well), and MC was added to cells (100 μg mL^{-1}) under the influence of a magnetic field. The intracellular uptake was quantified by flow cytometry. (c) Schematic representing the direction of the applied magnetic field.

6. Endocytosis inhibition

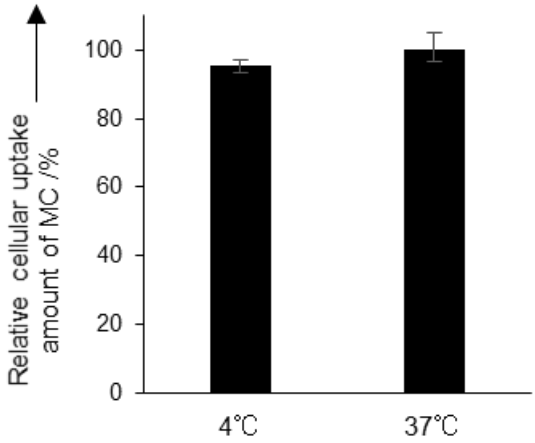

Figure S4. Intracellular uptake inhibition experiment. HeLa cells were seeded on 12-well plates (1.0×10^5 cells/well, and three independent experiments were performed in triplicate). The seeded cells were treated with MC under a magnetic field at 4°C or 37°C for 24 h. Cells were trypsinized and redispersed in staining buffer. The cellular uptake efficiencies of MC were quantified by flow cytometry. The cellular uptake efficiencies were normalized by the intensity of rhodamine B from MC at 37°C.

7. Protein exchange reaction

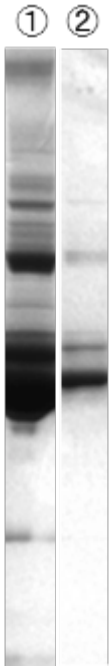

Figure S5. Complexation of serum proteins in FBS with MC via an exchange reaction evaluated by SDS-PAGE. The MC/BSA complex (MC, 100 μg mL^{-1}; BSA, 17 μg mL^{-1}) interacted with 10% FBS. The MC/BSA complex, which were magnetically separated from FBS, were treated with sodium dodecyl sulfate with heating at 70°C. The electrophoresis was carried out using a 7.5% polyacrylamide gel (20 mA, 70 min). The gel was stained with Coomassie brilliant blue (CBB). Lanes 1 and 2 indicate 10% FBS and the magnetically isolated MC/BSA complex after interaction with FBS, respectively.

8. Insulin delivery with MC

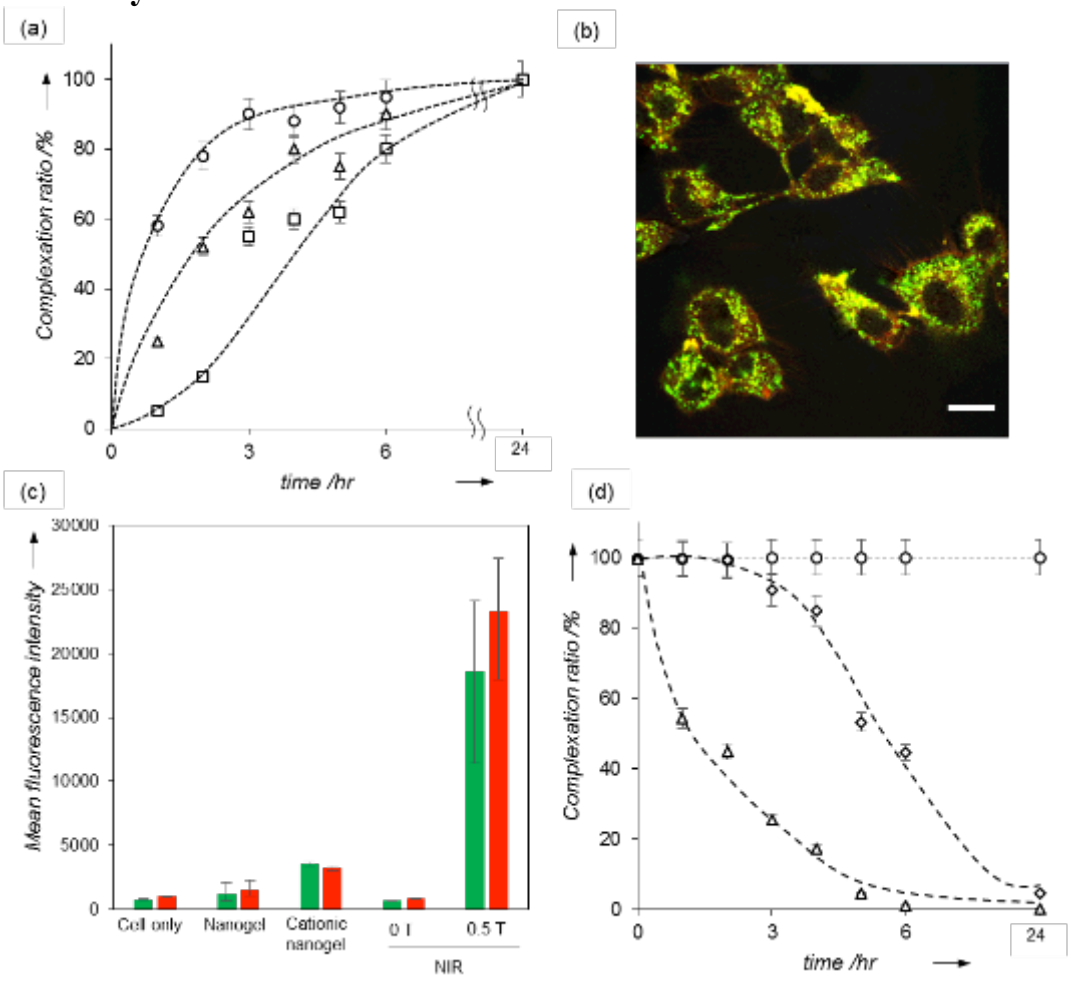

Figure S6. (a) Complex formation with FITC-labeled insulin. MC (100 μg mL^{-1}) and FITC-insulin (14 μg mL^{-1}) were mixed in PBS. The complexation ratio (%), the relative amount of free protein to total protein, was quantified by measuring the fluorescence intensity from the free insulin isolated from the complex by magnetic separation. Three independent experiments were performed in triplicate. (b) Cell internalization of MC/FITC-insulin complexes. CLSM images of HeLa cells after 24 h incubation with rhodamine B (red)-labeled MC/FITC-labeled insulin (green) in the absence of a magnetic field. The scale bar indicates 20 μm. (c) The mean fluorescence of rhodamine-labeled MC and FITC-labeled insulin accumulated in HeLa cells was measured by flow cytometry after 24 h incubation of cells with MC−1/FITC-insulin complexes. Three independent experiments were performed in triplicate. (d) Protein release in the presence of a highly concentrated protein solution, mimicking the intracellular environment using serum proteins. After complexation with insulin, PBS (●) or FBS (10%◆, 20%▲) was added to the complex and the ratio of incorporated insulin was calculated by measuring fluorescence intensity of the free insulin isolated from the complex by magnetic separation. Three independent experiments were performed in triplicate.

9. Protein transduction

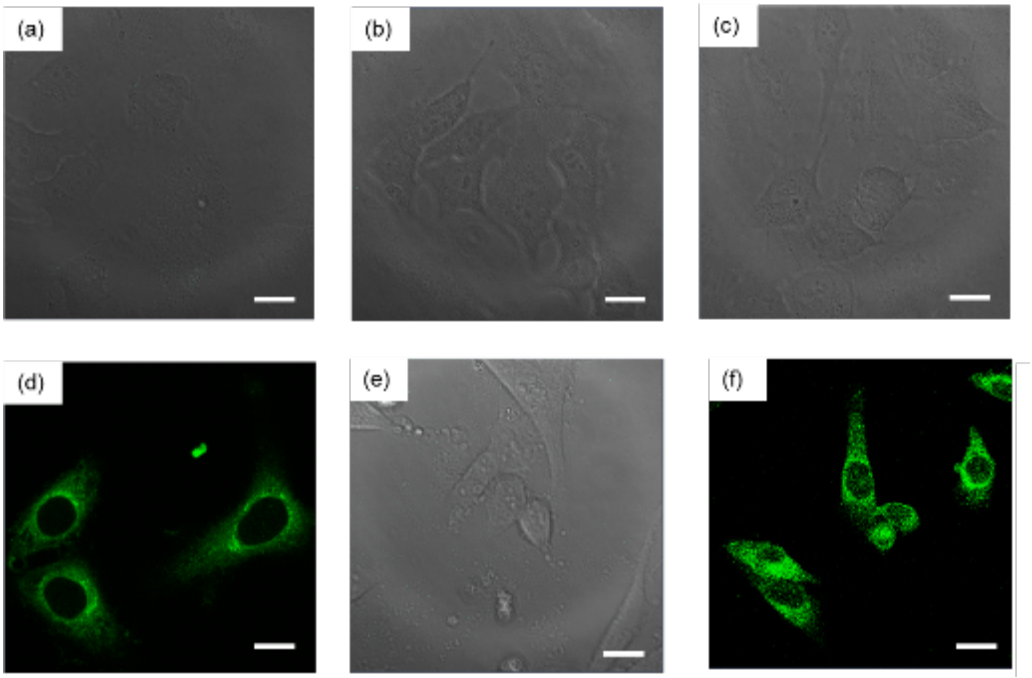

Figure S7. Confocal laser scanning microscopic (CLSM) image of HeLa cells incubated without treatment (a), with free β-galactosidase (b), nanogel (CHP)/β-galactosidase complex (c), cationic nanogel (CHP-NH_2)/β-galactosidase complex (d) MC/β-galactosidase complex without a magnetic field or MC/β-galactosidase complex with a magnetic field for 24 hr. Tokyo-green-β-gal (10 μM) was added to HeLa cells before CLSM observation. The concentrations of CHP, CHP-NH_2 and MC were fixed at 10 μg mL^{-1}.

10. Enzymatic activity of delivered protein within cells

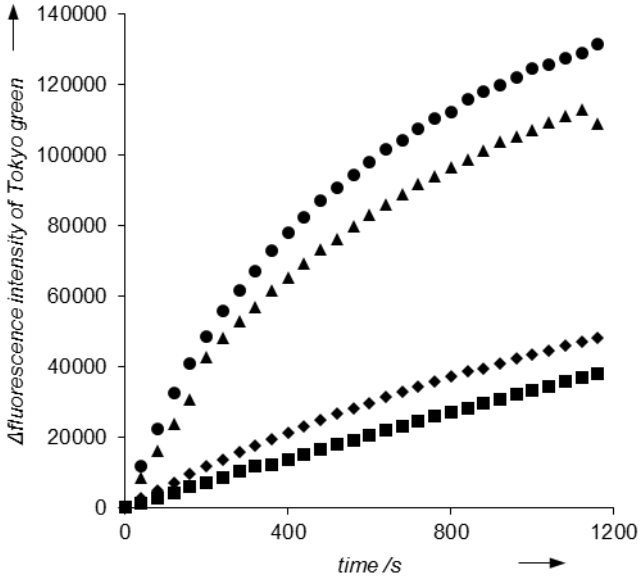

Figure S8. Enzymatic activity of β-galactosidase within cells. HeLa cells were treated with a MC1/β-galactosidase complex (MC1, 10 μg mL^{-1}; β-galactosidase, 0.042 μg mL^{-1}). After administration of this complex, Tokyo green β-gal (10 μM) was also added to the cells. Tokyo-green fluorescence was monitored for the first 20 min, after incubation for 0 h (circles), after 24 h (triangles) after 48 h (rhombuses) and after 72 h (squares). Six independent single experiments were performed.

Table S3. Relative enzymatic activity of β-galactosidase delivered to HeLa cells with a MC1/β-galactosidase complex (MC1, 10 μg mL^{-1}; β-galactosidase, 0.042 μg mL^{-1}). After administration of this complex, Tokyo green β-gal (10 μM) was also added to cells. The relative enzymatic activity was quantified by the slope of the change in intensity of Tokyo-green fluorescence, measured over 20 min, after the indicated incubation times.

Time (h)	Relative enzymatic activity (%)
0	100
24	50
48	17
72	8

11. Cytotoxicity of 5-fluorouridine analogue and 5-fluorouridine-*O*-β-galacto-pyranoside

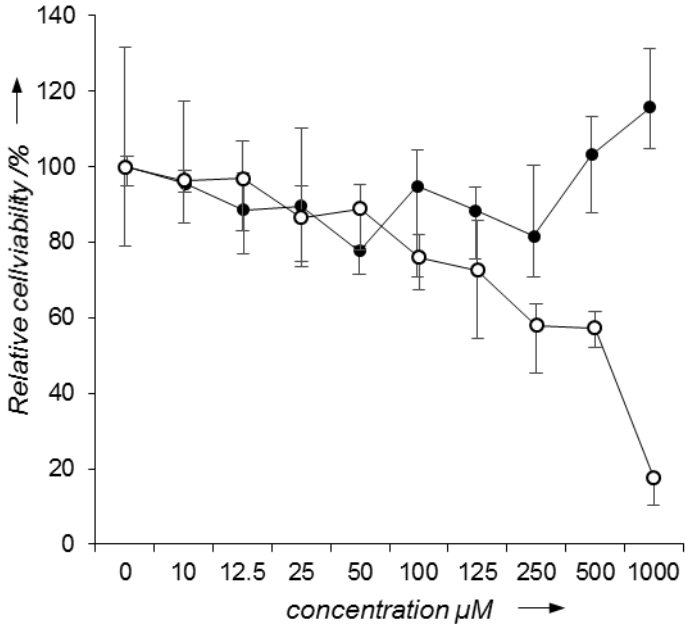

Figure S9. Cytotoxicity of 5-fluorouridine (5-FUR, open circles) and 5-fluorouridine -*O*-β-galactopyranoside (5-FUR-β-gal, closed circles) toward HeLa cells when incubated for 24 h. Three independent experiments were performed in triplicate.

12. Apoptosis detection assay

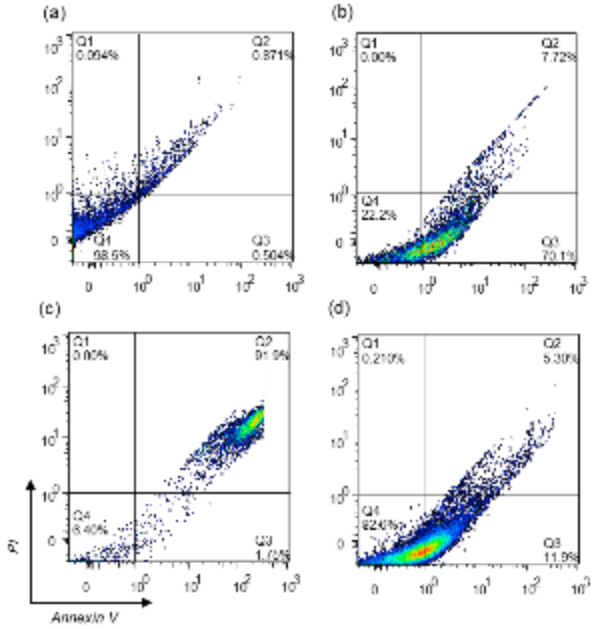

Figure S10. Apoptosis detection assay; annexin-V/PI staining. The stages of apoptosis were identified by Annexin-V/PI staining. Non-treated CT26 cells (a). CT26 cells treated with a MC/caspase-3 complex (50 nM, b; 100 nM, c) with or without a magnetic field (100 nM, d) for 24 h.

References

[1] Y. Tahara, SA. Mukai, S. Sawada, Y. Sasaki, and K. Akiyoshi, *Advanced Materials*, **2015**, 27, 5080-5088.

[2] K. Katagiri, K. Ohta, K. Sako, K. Inumaru, K. Hayashi, Y. Sasaki, and K. Akiyoshi, *ChemPlusChem*, **2014**, 79, 1631-1637.